

# Coupling efficiency of optics in single-mode fiber components

R. E. Wagner and W. J. Tomlinson

Many single-mode fiber components include some form of optics, such as lenses or mirrors, for collecting light from a source fiber or laser and concentrating it on a receiving fiber. For such components there is a direct and simple relationship between coupling efficiency and optical aberrations. This paper combines fiber-coupling fundamentals, classical optics, and diffraction theory to provide a compact description of coupling efficiency that includes the effects of aberrations, fiber misalignments, and fiber-mode mismatch.

## I. Introduction

In response to rapid advances in optical fiber technology, workers around the world are developing a wide variety of passive optical components, such as couplers, switches, and wavelength multiplexers, for manipulating and processing the signals in fibers; and significant interest in single-mode fibers and long-wavelength laser diodes has created a need for such components that can be used with single-mode fibers. Most of these components include some form of optics, such as lenses or mirrors, for collecting light from a source fiber or a laser and concentrating it on a receiving fiber or fibers.

These components always exhibit optical-coupling loss, which is completely determined by the degree to which the optics depart from ideal, that is, by the aberrations and misalignments of the optical system. This means that a component designer, in the process of optimizing coupling efficiency, can make beneficial use of the enormous body of knowledge that already exists concerning classical optical imaging systems.

This paper develops the relationship between optical aberrations and coupling efficiency for single-mode fiber components. The result provides a compact description of coupling efficiency and includes the effects not only of aberrations but also of fiber misalignments

and of fiber-mode mismatch. It is equally applicable to fiber-to-fiber coupling and to laser-to-fiber coupling. Although the present analysis is restricted to single-mode fiber components, similar techniques are applicable to multimode components.

In Sec. II there is an overview of the optical-coupling problem including a general description of the problem, an outline of the steps involved in its solution, the basic result, and noteworthy features of the result. This is followed by a series of definitions that establish the similarities and differences between the coupling problem and classical optical imaging, and then by a more formal development that is based on rigorous diffraction theory. However, the formal development emphasizes a qualitative understanding of the problem and solution, leaving many of the details for an appendix.

In the remaining sections the basic results are used to calculate coupling efficiency for some practical situations that arise in component design. These include the effects of fiber misalignments, third-order aberrations, and random wave front perturbations. In some cases the calculations involve numerical evaluation of an integral, but in several cases the solutions are in closed form.

## II. Overview

The basic problem, illustrated in Fig. 1, is to calculate the power-coupling efficiency between two fibers, or a laser and a fiber, coupled by an optical system. Light diverging from a source fiber (or laser), located at the left of the figure, passes through the optical system, which may consist of lenses and other elements. These convert the diverging beam into a converging beam that forms an aberrated image of the source fiber (or laser). A receiving fiber is located near the image, so some of the beam is coupled into the receiving fiber. The problem, then, is to relate the power-coupling efficiency

The authors are with Bell Laboratories, Holmdel, New Jersey 07733.

Received 16 January 1982.  
0003-6935/82/152671-18\$01.00/0.  
© 1982 Optical Society of America.

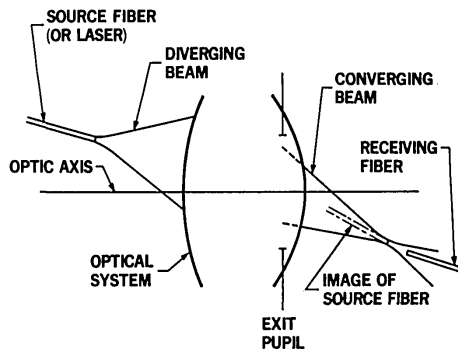


Fig. 1. Coupling from a source fiber (or laser) to a receiving fiber through a general optical system. The receiving fiber lies near an image of the source fiber.

to the fiber positions and characteristics and to the classical optical system properties.

The analysis is independent of whether the source is a fiber or a laser so, for simplicity, the balance of this paper only refers to the source as a fiber.

Although the fiber-coupling efficiency problem is similar in many respects to the classical optical imaging problem, there is an important difference. This difference is that the single-mode source fiber, lens, and receiving fiber together comprise a coherent system, rather than an incoherent system with a Lambertian source as is most often encountered in classical optics. This means that field distributions and the coherent optical transfer function are of primary concern, rather than irradiance distributions and the incoherent optical transfer function. Despite this difference, much of the insight gained from classical optics can be directly applied to the coupling efficiency problem.

In principle, it is possible to make a lossless passive component that will provide perfect coupling to the receiving fiber provided the source radiates into a single spatial mode of the radiation field. However, it is not possible to provide lossless coupling to a single-mode receiving fiber if the source radiates into more than one mode (the classical Lambertian source is an extreme example of this), or even if the source always radiates into a single mode but not always into the same spatial mode.

Formally, the coupling efficiency relationships are developed in a series of steps that correspond to determining the field distributions of the light at various planes in the optical system (see Fig. 2). The field distribution on the source plane, which is located at the end of the source fiber, is closely related to the mode pattern of the fiber. From this source field, diffraction theory is used to determine the field that would exist at an artificial plane within the optical system, called the entrance-pupil plane.

The field distribution at a second such plane, called the exit-pupil plane, is then determined as a transformation of the entrance-pupil field distribution. The transformation is governed by the ideal paraxial imaging properties of the optical system and by the coherent optical transfer function, a multiplicative term that

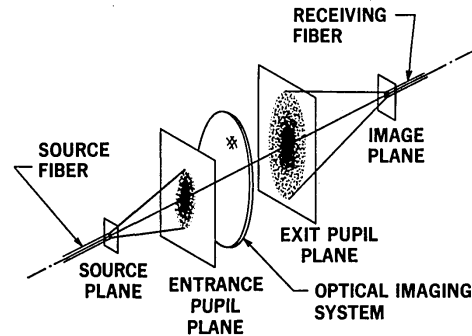


Fig. 2. Overview of the geometry involved in fiber-to-fiber (or laser-to-fiber) coupling through an optical imaging system. Four planes are important: the source and image planes containing the two fiber endfaces, and the entrance- and exit-pupil planes of the optical system.

describes the imperfections, or aberrations, of the optical system.

The exit-pupil field distribution produces an image field distribution, again calculated by diffraction theory, at the image plane located at the endface of the receiving fiber. The power-coupling efficiency is then the squared modulus of the overlap integral of the image field distribution and the mode pattern of the receiving fiber.

Conceptually, this description of coupling efficiency is convenient because it corresponds directly to the propagation of light through the optical system from source fiber to receiving fiber. The result, however, involves the evaluation of a triple integral—one for the overlap and one for each of the two diffraction calculations. For computational purposes the overlap integral can be transformed to any other convenient plane in the optical system. If it is transformed to the exit pupil plane, the power-coupling efficiency  $T$  can be expressed as a single integral with an integrand that is the product of three simple terms: the far-field distribution of the source-fiber mode pattern  $\Psi_S$ , the far-field distribution of the receiving-fiber mode pattern  $\Psi_R$ , and the coherent transfer function of the optical system  $L$ .

$$T = \left| \int \Psi_S L \Psi_R^* da \right|^2 \quad (1)$$

In Eq. (1) the three terms  $\Psi_S$ ,  $\Psi_R$ , and  $L$  are all directly measurable quantities and are related to fiber and optical system parameters in a familiar way. As a consequence the overlap integral expressed in the exit pupil most easily provides insight into the coupling efficiency problem and is most convenient for coupling efficiency calculations.

Several features of this result are particularly noteworthy. First, a single simple formulation accounts for lens aberrations, fiber misalignments, and mechanical alignments of the various device components. Even complicated effects such as nonflat fiber endfaces can be included if the appropriate far-field distribution is used. Second, when the calculations are performed at the exit pupil of the optical system, only one integration is required instead of three. This is because the two diffraction integrals that relate the source field distri-

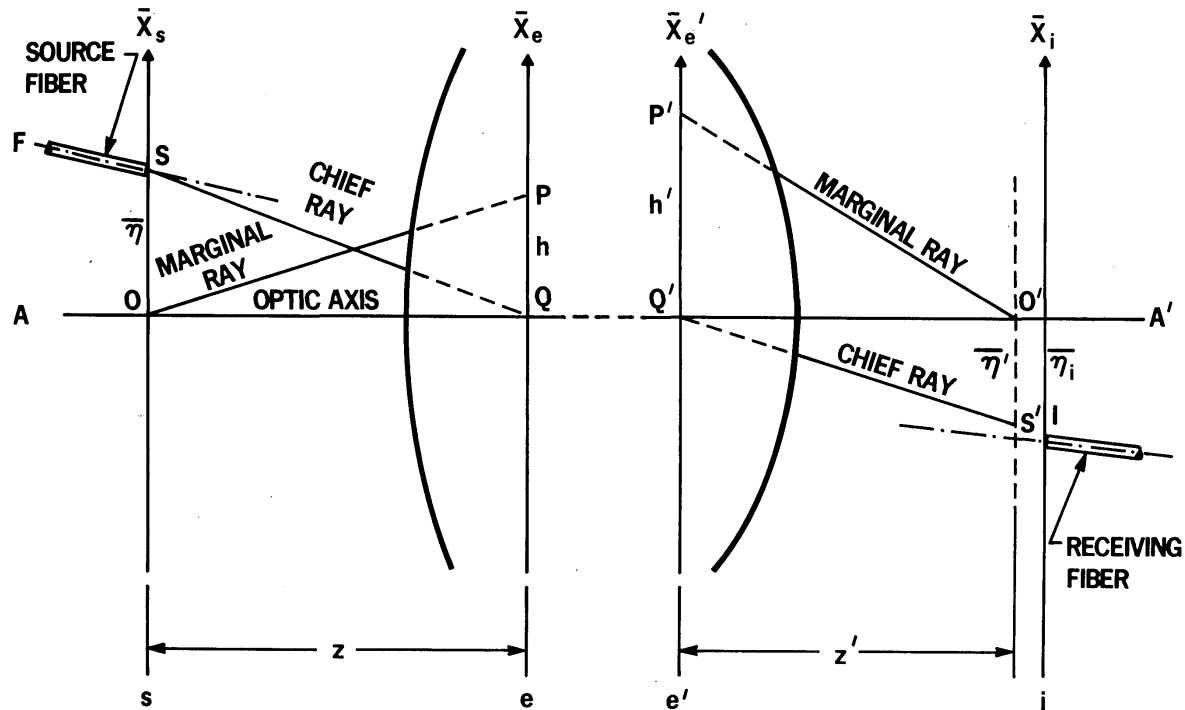


Fig. 3. Details of the geometry for analysis of the coupling-efficiency problem illustrating the first-order properties of the optical system. Included are the source-fiber position  $S$ , its image position  $S'$ , and the nearby receiving-fiber position  $I$ . Also shown are the source plane ( $s$ ), the entrance-pupil plane ( $e$ ), the exit-pupil plane ( $e'$ ), the receiving-fiber image plane ( $i$ ), and appropriate points and coordinates in those planes.

bution to the image field distribution are eliminated. Third, all three factors involved in the coupling efficiency integral are directly measurable experimentally, using various scanning and interferometric techniques. This permits a direct comparison between experimental and theoretical results. Fourth, the far-field distributions, which are needed for the coupling efficiency calculations in the exit pupil, are easier to measure than the actual mode patterns of the fibers, which would be needed if the calculations were to be considered as a triple integral at the image plane. Finally, the formulation presents a clear and simple understanding of how various imperfections will affect coupling efficiency.

### III. Definitions

To be useful in the context of classical optics, the formal development which follows in Sec. IV must be based on geometrical constructions that are consistent with accepted conventions. These conventions, which involve the source plane, the entrance- and exit-pupil planes, the image plane, and the aberrations, are reviewed in this section, emphasizing the similarities and differences between the fiber-coupling case and classical optics. A list of the symbols used in this paper, and their definitions, is given in Appendix B. For readers who are interested in a more complete description of classical optical analysis techniques we recommend the books by Born and Wolf,<sup>1</sup> and Welford.<sup>2</sup>

#### A. Source and Image Planes

As a visual aid for the definitions that follow, refer to

the sketch of Fig. 3. This sketch contains two arbitrarily positioned fibers and an optical system represented schematically by its first and last surfaces with all internal surfaces omitted. The optic axis is  $AA'$ , and the center of the source- and receiving-fiber endfaces are  $S$  and  $I$ , respectively. The point  $S$ , located on the source-fiber endface, has a paraxial image  $S'$  which lies near the receiving fiber. The point  $I$ , located on the receiving fiber, does not necessarily coincide with the paraxial image point  $S'$ , because the receiving fiber may not be perfectly aligned with the paraxial image  $S'$ . The source plane  $s$  contains the point  $S$ , while the image plane  $i$  contains the point  $I$ ; both planes are perpendicular to the optic axis  $AA'$ . The image plane is defined to contain the point  $I$  and not  $S'$ , because coupling calculations involve the field distribution that exists at the fiber endface.

The displacements from the optic axis of the points  $S$ ,  $S'$ , and  $I$  are represented by the vectors  $\vec{\eta}$ ,  $\vec{\eta}'$ , and  $\vec{\eta}_i$  respectively, with corresponding magnitudes  $\eta$ ,  $\eta'$ , and  $\eta_i$ .

#### B. Aperture Stop

The stop is important in classical imaging systems because it affects imaging properties of the system. In the fiber-coupling case some of this importance is lost, although the stop still serves as a useful reference for the definition of the entrance- and exit-pupil planes and the system aberrations.

The stop is an aperture within the system that physically limits the size of the cone of light that is ac-

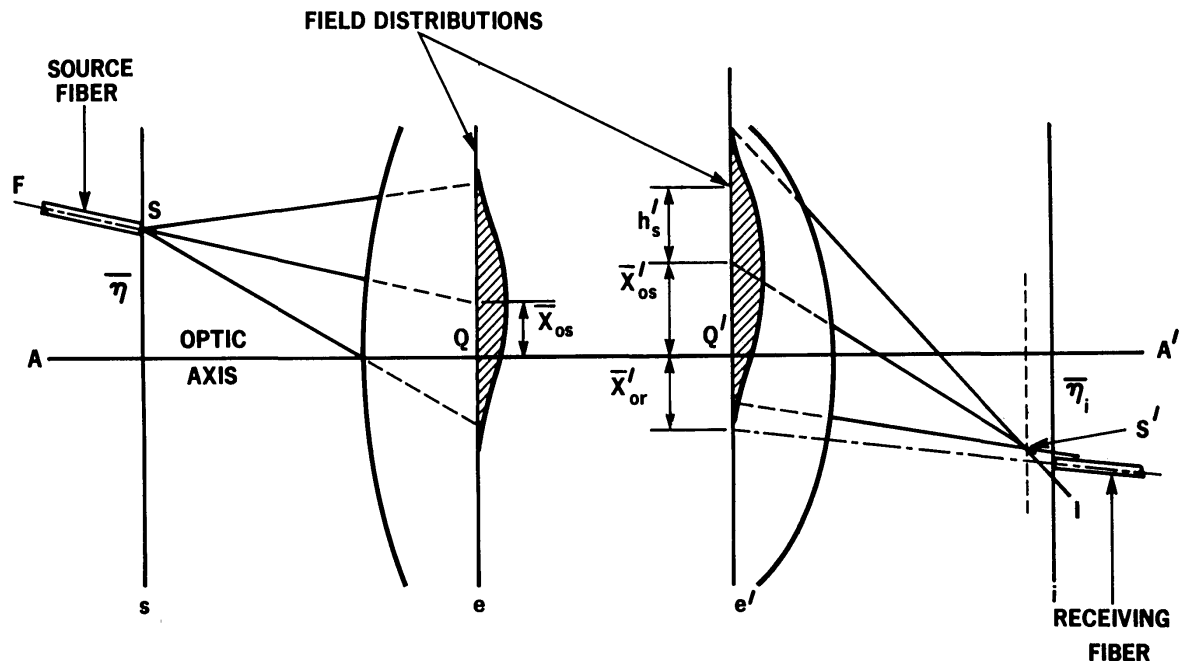


Fig. 4. Geometry for the fiber-coupling analysis, illustrating the source-fiber field distributions that occur in the entrance-pupil ( $e$ ) and exit-pupil ( $e'$ ) planes. These distributions may be de-centered by the amounts  $\bar{X}_{os}$  and  $\bar{X}'_{or}$  if the source-fiber axis is not directed toward the center of the entrance pupil.

cepted from any point on the source plane. In particular, one of the lens components, or an aperture deliberately introduced for this purpose, limits the light from the axial point  $O$ , which is the intersection of the optic axis and the source plane. This particular element is called the stop.

In classical optical systems, where the stop is smaller than the cone of light from the source, the size and location of the stop offer some measure of control on image quality, because these affect both optical system throughput and the aberrations. By contrast, the stop in single-mode fiber-coupling systems is ordinarily large enough that it does not physically restrict the beam, since the goal is to couple as much light as possible from one fiber to the other, and coupling efficiency cannot be increased by removing light.

Since the fiber characteristics, rather than the stop itself, set the angular spread and hence the physical extent of the beam, the location of the stop is somewhat arbitrary. As defined, however, it is consistent with the established convention in classical optics and, therefore, also useful for establishing the entrance- and exit-pupil planes and the system aberrations for the fiber-coupling case. Also, with this definition of the stop, its position does not depend on the characteristics or orientation of the input fiber, so that the aberrations of the optical system can be defined and measured without reference to the particular fiber configuration.

### C. Entrance- and Exit-Pupil Planes

The entrance and exit pupils are two artificial planes that allow the imaging properties of the optical system

to be described without direct reference to the actual lens surfaces or the stop. The entrance and exit pupils are images of the stop as seen from the source and receiving sides of the optical system, respectively. They are represented in Fig. 3 by the planes  $e$  and  $e'$ , and these two planes are scaled images of each other.

Two rays, the marginal and the chief, define the connection between the source and entrance-pupil planes and an analogous connection between exit-pupil and image planes. The marginal ray  $OP$ , and its image  $P'O'$ , originates at the axial point  $O$  and passes through the edge of the stop. This ray defines the numerical aperture (N.A.) of the optical system and the pupil magnification. The chief ray, so called because it is the central ray for the cone of light accepted by the system, originates at an off-axis point, such as  $S$ , and passes through the center of the stop. (If the source fiber location  $S$  coincides with the axial point  $O$ , some other point on the source plane must be chosen to define the chief ray. The choice is completely arbitrary.) This ray defines the lateral magnification of the system.

Since the entrance and exit pupils are images of the stop, the chief ray also passes through their centers,  $Q$  and  $Q'$ . Ordinarily the distribution of light in the exit pupil is controlled by the stop, which is usually centered on the optic axis. In the fiber-coupling case, however, the source fiber controls the distribution of light in the exit pupil as shown in Fig. 4, and this distribution is not necessarily centered in the exit pupil.

It is well to remember that both the entrance-pupil plane  $e$  and the exit-pupil plane  $e'$  are artificial constructs. Their locations are fixed, however, by the ac-

tual lens surfaces which determine the paths of rays through the system. In what follows, the first-order imaging characteristics and the optical aberrations are completely described in terms of these artificial planes  $e$  and  $e'$  without direct reference to the stop position or actual lens surfaces.

#### D. Coordinate System

For diffraction calculations a coordinate system is established in which the  $z$  axis is the optic axis  $AA'$ . It is convenient to define four independent coordinate systems corresponding to each of the four planes, all with a common  $z$  axis. The vectors  $\bar{X}_s, \bar{X}_e, \bar{X}_{e'}$ , and  $\bar{X}_i$  denote  $(x,y)$  coordinates in these systems, where the subscripts refer to the source plane, the entrance-pupil plane, the exit-pupil plane, and the image plane, respectively (see Fig. 3).

#### E. First-Order Imaging Properties

The optical properties of interest are the image and pupil magnifications, because these determine the location of the image and the extent of the converging wave in the exit pupil for a given source-fiber position and N.A. The image magnification  $m$  is  $\eta'/\eta$ , where  $\eta$  and  $\eta'$  are the distances from  $S$  and  $S'$  to the  $z$  axis, respectively (see Fig. 3). The pupil magnification  $m_e$  is  $h'/h$ , where  $h$  and  $h'$  are the distances from the points  $P$  and  $P'$  to the optic axis, respectively. The pupil magnification can alternately be expressed as  $m_e = \eta/\eta' \cdot z'/z = z'/(mz)$ , where  $z$  and  $z'$  are the distances from plane  $s$  to  $e$  and from plane  $e'$  to the paraxial image plane, respectively.

#### F. Wave-Front Aberrations

The wave-front aberrations of the optical system represent perturbations of the system from its first-order characteristics. These aberrations are expressed in the exit pupil as shown in Fig. 5. The wave-front aberrations are defined as the optical path difference  $W(\bar{X}_e)$  between the actual wave-front  $\Sigma'$  existing in the exit pupil and an ideal spherical reference wave-front  $\Sigma$  that converges toward point  $I$ . The vertex of the reference wave-front  $\Sigma$  is taken at  $Q'$ , so the radius of the reference wave front is  $R_i = Q'I$ . The aberrations  $W(\bar{X}_e)$  are measured on the reference wave-front  $\Sigma$ , but at pupil coordinates  $\bar{X}_e$  projected onto the exit pupil  $e'$ . This definition of wave-front aberrations is consistent with that normally used in optical lens design programs, in which the reference sphere is taken to have infinite radius.<sup>3</sup> Such consistency requires, however, that  $R_i$  be sufficiently large, a restriction imposed for other reasons in the coupling efficiency analysis [see Appendix A, Eq. (A17)] and satisfied by virtually all practical single-mode lens-coupling systems.

For a perfect optical system a diverging spherical wave in the entrance pupil produces a converging spherical wave in the exit pupil. Even in this case, however, the wave-front aberrations  $W(\bar{X}_e)$  may not be zero, because the center  $I$  of the reference wave-front  $\Sigma$  does not necessarily coincide with the image point  $S'$  toward which the actual spherical wave-front  $\Sigma'$  con-

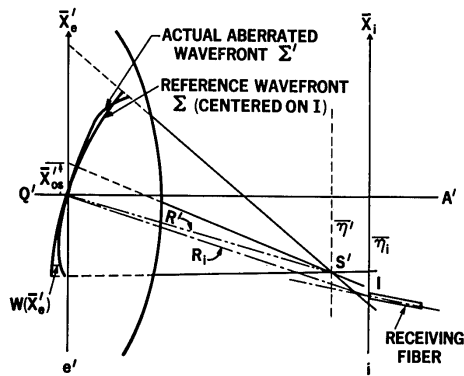


Fig. 5. Image-space geometry for the coupling-efficiency problem illustrating an ideal reference wave-front  $\Sigma$  that converges toward the receiving fiber (point  $I$ ) and the actual wave-front  $\Sigma'$  emerging from the exit pupil. The difference between the two is called the wave-front aberration  $W(\bar{X}_e)$ . Such aberrations cause a reduction in coupling efficiency because they represent an improper phase between the two distributions to be coupled.

verges. Such aberrations are real in the sense that they cause coupling losses at the receiving fiber and are characterized as fiber misalignment aberrations. If the optical system contains wave-front aberrations of its own, these contribute to the total wave-front aberrations as well. Both optical system wave-front aberrations and misalignment aberrations are described in the exit pupil, allowing both coupling effects to be handled simultaneously in a manner consistent with accepted convention in classical optics.

#### G. Coherent Optical Transfer Function

The coherent optical transfer function  $L(\bar{X}_e)$  relates the exit-pupil field distribution to the scaled entrance-pupil distribution. In the geometrical optics approximation it is given as  $L = \exp[-ikW(\bar{X}_e)]$ , where diffraction within the optics is neglected. The neglect of diffraction between the two pupil planes is the major simplifying assumption involved in this development. In many cases this approximation is sufficiently accurate, but in special cases, such as when the beam is extremely small or when the stop is far from the lens surfaces, diffraction within the optics must be considered.

#### H. Third-Order Aberrations

In classical optics it is quite often useful to express  $W(\bar{X}_e)$  as a polynomial expansion of the image height  $\eta'$  and of normalized exit-pupil coordinates  $\bar{X}_e/h'$ . The normalized exit-pupil coordinates are usually represented by polar coordinates  $(\rho, \phi)$ , where  $\phi$  is the angle measured from the plane that contains the optic axis  $AA'$  and the source point  $S$ .

For a symmetrical optical system the polynomial expansion for wave-front aberrations carried to the third-order is

# Explore Litigation Insights

Docket Alarm provides insights to develop a more informed litigation strategy and the peace of mind of knowing you're on top of things.

## Real-Time Litigation Alerts



Keep your litigation team up-to-date with **real-time alerts** and advanced team management tools built for the enterprise, all while greatly reducing PACER spend.

Our comprehensive service means we can handle Federal, State, and Administrative courts across the country.

## Advanced Docket Research



With over 230 million records, Docket Alarm's cloud-native docket research platform finds what other services can't. Coverage includes Federal, State, plus PTAB, TTAB, ITC and NLRB decisions, all in one place.

Identify arguments that have been successful in the past with full text, pinpoint searching. Link to case law cited within any court document via Fastcase.

## Analytics At Your Fingertips



Learn what happened the last time a particular judge, opposing counsel or company faced cases similar to yours.

Advanced out-of-the-box PTAB and TTAB analytics are always at your fingertips.

## API

Docket Alarm offers a powerful API (application programming interface) to developers that want to integrate case filings into their apps.

## LAW FIRMS

Build custom dashboards for your attorneys and clients with live data direct from the court.

Automate many repetitive legal tasks like conflict checks, document management, and marketing.

## FINANCIAL INSTITUTIONS

Litigation and bankruptcy checks for companies and debtors.

## E-DISCOVERY AND LEGAL VENDORS

Sync your system to PACER to automate legal marketing.